Journal of Biomechanics

Numerical Simulation of Transcatheter Mitral Valve Replacement the Dynamic Implication of LVOT Obstruction in the Valve-In-Ring Case

--Manuscript Draft--

Manuscript Number:	BM-D-22-00565R2
Article Type:	Full Length Article (max 3500 words)
Keywords:	Transcatheter Mitral Valve Replacement; Living Heart Human Model; Finite Element (FE) Analysis; Computational Fluid Dynamic (CFD)
Corresponding Author:	Salvatore Pasta, Ph.D. University of Palermo Palermo, ITALY
First Author:	Salvatore Pasta, Ph.D.
Order of Authors:	Salvatore Pasta, Ph.D.
	Chiara Catalano
	Stefano Cannata
	Julius M. Guccione
	Caterina Gandolfo
Abstract:	Transcatheter mitral valve replacement (TMVR) has been used for “off-label” treatment when annuloplasty band ring for mitral repair fails. However, the complex anatomy and function of the mitral valve may lead to fatal complications as a result of the left ventricular outflow tract (LVOT) obstruction in TMVR. We report the structural and hemodynamic response of LVOT obstruction resulting from TMVR with the Edwards SAPIEN 3 Ultra (S3) device. We modified the original Living Heart Human Model (LHHM) to account for a failed mitral valve with an annuloplasty band ring and simulated the cardiac beating condition in the setting of S3 device implantation. Findings demonstrated a high dynamic behavior of the newly formed LVOT (neo-LVOT) as confined by the displaced mitral valve and the interventricular septum. During the cardiac beat, the neo-LVOT area oscillated from a maximum of 472.1 mm 2 at early systole to the minimum of 183 mm 2 at end-systole. The profile of both anchoring force and contact pressure revealed that the band ring serves as the anchoring zone while mitral valve is primally displaced by the deployed device. At early systole, computational flow dynamics highlighted hemodynamic disturbances associated with the LVOT obstruction, with a skewed flow towards the septum and a pressured drop of 4.5 mmHg between the left ventricular apex and the neo-LVOT region. This study can lead to a more accurate assessment of the risk induced by the LVOT obstruction when stratifying patient anatomic suitability for TMVR.

Università degli Studi di Palermo

Dear Editor,

The present paper shows a computational study to assess the feasibility to transcatheter mitral valve replacement as considered as off-label application of commercial devices.

This study adoptes a realistic cardiac simulator as the living heart project and is supported by THV manufacturer.

All authors were fully involved in the study and preparation of the manuscript which contribution originality can be confirmed by members of University Collage San Francisco and the University of Palermo . All authors approve the submission.

The manuscript, or part of it, has neither been published (except in form of abstract or thesis) nor is currently under consideration for publication by any other journal.

we kindly suggests the name of few reviewers as expert on the field

Best Regards,

Reviewer #2

We thank the reviewer for his or her valuable comments to our paper. The comments were constructive and have led to a remarkable improvement of the manuscript. We have attempted to maximize the utility of these comments and hope that the revised version of the paper addresses all the comments raised. All comments are highlighted in yellow with respect to previous version.

General comment

In this revision, the authors definitely improved the manuscript by including more details in the text. However, one of my comments, that the paper shows only one model of a specific case with no comparative study (comment 2), was not really addressed. I totally agree that this model cannot be validated, but parametric studies are feasible, and they can at least predict some clinically useful trends. I gave the authors several ideas on how to make the results of this model more meaningful, and at least one of those ideas is very straight-forward to implement (in comment 3, changing material properties of the device does not require any modification to the geometry/mesh). I understand the authors' preferences to investigate such changes in the future, but I still think that their decision makes this study much less interesting and useful than it could have been. I strongly encourage the authors to expand the scope of their current paper by adding such a simple model. It will vastly improve the paper and make it suitable for publication.

Reply: we thank the reviewer for encouraging us in performing additional simulations and believes that this has strongly improved the quality of the manuscript, if the reviewer agrees.

Specifically, we added the results of n.3 additional simulation on the resulting structural performance of the S3 Ultra device. These new simulations are:

1. A first model with a stiff band ring as opposed to the nitinol band ring as kindly suggested by the reviewer
2. A second model with an increased amount of balloon fluid-filling volume to simulate the device overexpansion that may be performed in the clinical setting
3. A third model with a translated device to simulate a change in the implantation depth.

In brief, we observed that the stiff band ring reduced the neo-LVOT area at diastole and systole but the highest reduction was observed with balloon overexpansion. In a different way, the high implantation depth determined high neo-LVOT area but slightly low contact pressure in the mitral valve leaflet. The results of such simulations were added, please see the new Table 2 and Figure 8. Several sentences were added in each section to describe these simulations and are here re-written:

Introduction: the following sentence was added in the last paragraph

“A comparative study was carried out by changing the material properties of the band ring, simulating the balloon overexpansion and altering the implantation depth.”

Section 2.1:

“An additional model was developed by changing the material behavior of the band ring to simulate the TMVR in a stiff band ring. Specifically, the band ring was simulated as a rigid material while other material descriptors of LHHM and S3 Ultra system were not changed. ”

Section 2.3:

“To further investigate the interaction of the S3 Ultra with the human host, the case of a high implantation depth in the left atrium was also investigated. This was obtained by translating the device and implantation system of 5 mm in the left atrium.”

and

“Balloon overexpansion may occur in clinical setting to increase the device adherence to the band ring. In this way, an additional simulation was developed increasing the fluid volume of 1 ml with respect to the reference one.”

Results

“The comparative study using the stiff band ring, high implantation depth and balloon overexpansion highlighted different TMVR simulation outcomes (Fig. 7). Table 2 summarizes the changes of neo-LVOT area and contact pressure with respect to the reference LHHM model. “

Table 2: Comparison of neo-LVOT area values among different parametric models

	Neo-LVOT area (mm^2)		Contact Pressure (MPa)	
	Max	Min	Ring	Mitral Valve
Reference Model	472.1	183.0	28.2	26.7
Stiff Band Ring	455.8	165.7	41.6	32.5
Balloon Overexpansion	434.6	151.4	32.8	29.4
High Implantation Depth	495.6	201.2	30.5	22.3

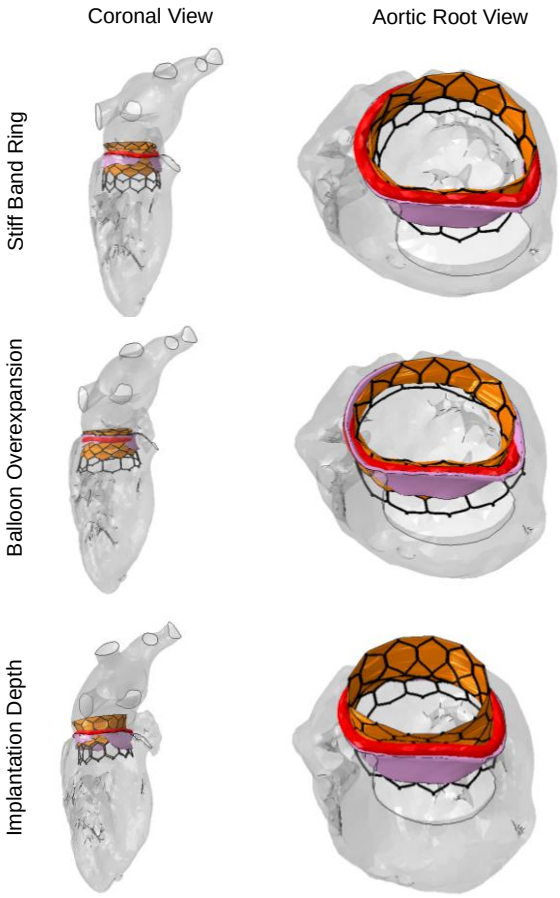

Fig 8 Changes in the TMVR simulations in case of a stiff band, balloon overexpansion and high implantation depth.

Discussion:

“The comparative study demonstrated that role of band ring material properties, device overexpansion and suboptimal implantation depth on the resulting device performance. Low magnitude of neo-LVOT area at systole and diastole were found for the stiff band ring and balloon overexpansion, with lowest area measurements when the fluid-filling volume was increased. In a different way, a shift of the implantation depth towards the left atrium led to larger neo-LVOT area but lower contact pressure on the mitral valve than that shown by the reference model following manufacturer guidelines”

Conclusion:

Future studies in patient-specific geometries including different mitral valve morphologies different sizes of mitral valve leaflets and stiff versus flexible band rings will help to achieve better translational clinical value by enhancing the pre-TMVR planning in borderline patient anatomy.

Numerical Simulation of Transcatheter Mitral Valve Replacement: the Dynamic Implication of LVOT Obstruction in the Valve-In-Ring Case

Salvatore Pasta[1,2], Chiara Catalano[1], Stefano Cannata[3], Julius M. Guccione[4], Caterina Gandolfo[3]

[1]Department of Engineering, Viale delle Scienze, Università degli Studi di Palermo, Palermo, Italy.

[2] Department of Bioengineering Research, IRCCS-ISMETT, Palermo, Italy.

[3] Department for the Treatment and Study of Cardiothoracic Diseases and Cardiothoracic Transplantation, IRCCS-ISMETT, Palermo, Italy.

[4] Department of Surgery, University of California San Francisco, San Francisco, CA, United States.

*** Correspondence:**

Salvatore Pasta, PhD
Professor of Industrial Bioengineering,
Department of Engineering
University of Palermo
Phone: +39 091 3815681
FAX: +39 091 3815682
e-mail: salvatore.pasta@unipa.it

Abstract

Transcatheter mitral valve replacement (TMVR) has been used for “off-label” treatment when annuloplasty band ring for mitral repair fails. However, the complex anatomy and function of the mitral valve may lead to fatal complications as a result of the left ventricular outflow tract (LVOT) obstruction in TMVR. We report the structural and hemodynamic response of LVOT obstruction resulting from TMVR with the Edwards SAPIEN 3 Ultra (S3) device. We modified the original Living Heart Human Model (LHHM) to account for a failed mitral valve with an annuloplasty band ring and simulated the cardiac beating condition in the setting of S3 device implantation. Findings demonstrated a high dynamic behavior of the newly formed LVOT (neo-LVOT) as confined by the displaced mitral valve and the interventricular septum. During the cardiac beat, the neo-LVOT area oscillated from a maximum of 472.1 mm^2 at early systole to the minimum of 183 mm^2 at end-systole. The profile of both anchoring force and contact pressure revealed that the band ring serves as the anchoring zone while mitral valve is primally displaced by the deployed device. At early systole, computational flow dynamics highlighted hemodynamic disturbances associated with the LVOT obstruction, with a skewed flow towards the septum and a pressured drop of 4.5 mmHg between the left ventricular apex and the neo-LVOT region. This study can lead to a more accurate assessment of the risk induced by the LVOT obstruction when stratifying patient anatomic suitability for TMVR.

Keywords: Transcatheter Mitral Valve Replacement, Living Heart Human Model, Finite Element (FE) Analysis, Computational Fluid Dynamic (CFD)

Statements and Declarations

Funding: This study was funded by the grant “Sim4SAPIEN” from the Edwards Lifesciences SA (THV-I20-532).

1. Introduction

Mitral valve regurgitation is the most common valvular disease worldwide with a prevalence of 10% in the general population (Wu et al., 2018). A significant number of patients with mitral regurgitation are also at high risk for surgical repair as advanced age and comorbidities can lead to mortality ranging from 7.4% to 15.1% (Castillo-Sang et al., 2015). In the last few years, transcatheter mitral valve replacement (TMVR) has evolved considerably towards becoming an effective therapy in the setting of degenerated bioprostheses, failed annuloplasty band rings and mitral annular calcifications (Bapat et al., 2018; Muller et al., 2017). The positive outcome of TMVR procedure reported in recent studies (Muller et al., 2021; Whisenant et al., 2020) is partly due to clinician experience and confidence on performing the well-established transcatheter aortic valve replacement (TAVR). However, the current generation of transcatheter heart valves (THV) are not specifically designed for mitral valve repair and are therefore used as “off-label” applications in mitral implantations. As the THV is implanted in the diseased mitral valve, the native left ventricular out flow tract (LVOT) is extended into the left ventricle by generating a modified anatomic region (namely, the neo-LVOT). This region is confined to the permanently displaced THV and the native anterior mitral valve leaflet together with the interventricular septum. LVOT obstruction is the major complication after TMVR, with incidence rates ranging between 8.2% and 11.2%, and can ultimately lead to hemodynamic impairment and death (Babaliaros et al., 2021). Simulating TMVR is more challenging than simulating TAVR because the highly complex nature of mitral valve and its dynamic behavior mean that simulation must be performed on a beating heart model. There is therefore a limited literature on the computational modeling of TMVR. Computational fluid dynamic was adopted to quantify the stenotic sub-aortic flow alterations and the pressure drop induced by the prolonged THV protrusion as modeled by a rigid wall in the LVOT (Kohli et al., 2018). Similarly, a parametric analysis of the impact of THV extension in the LVOT has revealed an increase in the left ventricular afterload as the obstruction length is pronounced (De Vecchi et al., 2018). Recently, computational flow analysis was used to evaluate the effectiveness of mitral valve anterior leaflet laceration (ie, the LAMPOON mini-invasive surgery) for redistributing the flow patterns and ultimately mitigating the impact of the LVOT obstruction. These studies do not

perform structural simulations and thus have not investigated the interaction of the device with the human host. In this context, the Living Heart Human Model (LHHM) developed by Dassault Systemes is an extremely realistic and accurate multiphysics model of an adult beating heart, and is therefore the ideal cardiac tool to investigate the biomechanics of TMVR and the role of LVOT obstruction on patient outcomes. The simulation of the cardiac beat with the LHHM can reveal important insights in the THV post-deployment performance and ultimately offer a methodology to facilitate the optimal design of THVs for mitral valve repair and enhance pre-operative planning for improving the management of patient undergoing TMVR.

This study sought to assess the dynamic role of LVOT obstruction resulting from the TMVR simulation using the LHHM. For this, we adapted the LHHM to mimic the case of a patient who underwent transcatheter mitral valve-in-ring implantation. This was accomplished by changing the left ventricular material response to model the failed heart condition and then simulating the presence of the annuloplasty band ring. Next, the balloon-expandable Edwards SAPIEN 3 Ultra (S3) device (Edwards Lifesciences, USA) was virtually deployed in the LHHM to assess the anchoring device performance and the neo-LVOT area over the cardiac beat. A comparative study was carried out by changing the material properties of the band ring, simulating the balloon overexpansion and altering the implantation depth. Finally, a computational fluid dynamic analysis was carried out using the end-systolic LHHM deformed configuration to evaluate the sub-aortic flow and pressure drop in correspondence of LVOT obstruction.

2. Methods

The simulation study of TMVR in the failed annuloplasty band ring consisted of the following steps:

1. Adapting the original LHHM to account for a failed mitral valve by inhibiting the active contraction of the myocardial wall near the posterior papillary muscle.

2. Modeling the suturing of the annuloplasty band ring into the mitral annulus using wire connections and contact conditions.
3. Simulating the deployment of the S3 Ultra device by virtually inflating the balloon and then modeling the heartbeat of repaired mitral valve apparatus.
4. Computational flow analysis of the left heart hemodynamics to quantify the sub-aortic flow and pressure gradient near the LVOT obstruction.

2.1 Band ring and THV models

The band ring was derived from a prototype previously investigated by our group (Baillargeon et al., 2015) and is characterized by a nitinol annular material with cross-sectional circular geometry (d=3 mm). The original prototype was downscaled to accommodate the MV annulus of LHHM geometry, and then meshed with unstructured tetrahedral elements. For material properties, the constitutive law reported by Morganti and collaborators (Morganti et al., 2016) was used. An additional model was developed by changing the material behavior of the band ring to simulate the TMVR in a stiff band ring. Specifically, the band ring was simulated as a rigid material while other material descriptors of LHHM and S3 Ultra system were not changed.

In accordance with mitral annulus geometry of LHHM, the S3 Ultra with diameter of 23 mm was used in this study. Specifically, the S3 Ultra stent frame was modeled using micro-CT images and then meshed with nearly 60,000 structured hexahedral solid elements with reduced integration and hourglass control (Pasta et al., 2020a; Pasta et al., 2020b). To avoid mesh distortion and ensure solution convergence, the THV skirt was modeled after the crimping phase by closing the device frame cells at mid-thickness of the S3 frame geometry (Fig. 1B). Then, triangular shell elements with a thickness of 0.1 mm were used to model the sealing skirt during the S3 deployment. The constitutive model of the S3 metallic frame was a bilinear elasto-plastic material (ρ=8000 kg/m^3, E= 233 GPa, σ_Y=414 MPa, σ_{ult}=930MPa, ε_p=0.45 and ν=0.35) and the skirt had a perfect elasto-plastic model to account for the polyethylene terephthalate material (ρ=8000 kg/m^3, E= 55 MPa, σ_Y= σ_{ult}=6.6 MPa, ε_p=0.6 and ν=0.45) (Pasta et al., 2020a). For the THV, the valve leaflet geometry

assumed a parametric model with linear-elastic material properties (ρ=1060 kg/m^{3,} E=8 MPa and ν=0.45) as reported by Auricchio et al (Auricchio et al., 2014). Reverse engineering was used to acquire the balloon shape profile using a laser scanner (Hexagon Manufacturing Intelligence, Cobham, Great Britain), and then to revolve the generative curve around the balloon axis in the commercial software Rhinoceros, (Robert McNeel & Associates, USA). The balloon was discretized with membrane elements (M3D4) with thickness of 0.1mm and linear-elastic material properties (ρ=1060 kg/m^{3,} E=600 MPa and ν=0.3) (Bailey et al., 2016).

2.2 LHHM description

The LHHM developed by SIMULIA Living Heart Project (Fig. 1) is an advanced cardiac tool in which the geometry is a realistic and accurate representation of an adult male anatomy (Baillargeon et al., 2014). The LHHM includes all ventricular and atrial chambers, heart valves and major vessels (i.e., the aorta, pulmonary artery and vena cava) and the biomechanical response is governed by an electrical potential activating the contraction of myocardial wall. The coupling with a 1-D lumped parameter model allows one to consider the interaction between the circulating blood and the deforming myocardium and thus obtain the pressure-volume loop. Anatomical parts are meshed with tetrahedral elements and linear truss elements (only for chordae tendineae) for a total of 443,564 mechanical degrees of freedom.

In the LHHM, the electrical potential is first computed for the whole heart and then transferred to the mechanical model using both active contraction and passive material properties to simulate the cardiac beat. The active stress in the cardiac fiber direction is generated by a time-varying elastance model where the active force is a function of the current sarcomere length, peak intracellular calcium concentration, and fiber activation time. The passive behavior of heart chambers is modelled with the anisotropic hyperelastic constitutive model proposed by Ogden and Holzapfel (Holzapfel and Ogden, 2009), which has been widely used in several cardiac simulation studies (Guccione et al., 2001; Walker et al., 2005).

Since the current study was focused on the mitral function and the TMVR feasibility, additional attention was given to the mechanical properties of mitral valve leaflets and chordae. Specifically, the mitral valve was modeled using the following strain energy function with strain invariants I_1, I_{4f}, I_{4s}, and I_{8fs}:

$$\Psi_{dev} = \frac{a}{2b}\exp[b(I_1 - 3)] + \sum_{i=f,s}\frac{a_i}{2b_i}\{\exp[b_i((I_{4i} - 1)^2)] - 1\} + \frac{a_{fs}}{2b_{fs}}[\exp(b_{fs}I_{8fs}^2 - 1] \quad \text{Eq1}$$

The eight material parameters a, b, a_f, b_f, a_s, b_s, a_{fs}, b_{fs}, were fit using the biaxial mechanical characterization on the porcine aorta proposed by MayNewman and Yin (May-Newman and Yin, 1995).The chordae constitutive behavior chosen was hyperelastic with a Marlow form of strain energy potential using uniaxial test data from Kunzelmann and Cochran (Kunzelman et al., 1993). The chordae are coupled to the ventricular papillary muscles using tie constraints. In the LHHM, the mitral valve failure was obtained modifying the left ventricular material properties in the myocardial wall region near the posterior papillary muscle (see inset of Fig. 1A). Specifically, active contraction was deactivated in an element set near the papillary muscle during the cardiac beat to simulate a failed heart condition. The extension and position of the failed myocardial wall region was decided according to the pathological remodeling of the heart infarction as characterized by an ischemic area near the papillary muscle of the anterior left ventricular wall. The passive heart behavior constitutive law has the form shown by Eq.1. Thus, the dysfunction of the failed myocardial region was modeled by increasing the isotropic response of 30% as done previously (Guccione et al., 2003). Similarly, the end-systolic dysfunction was modeled by reducing the parameter representing the peak intracellular calcium concentration (C_{a0}) of 20%. Table 1 summarize the material parameters of the left heart, ischemic region and mitral valve. In the LHHM, the heart rate is fixed to 60 bpm resulting in a systolic phase of 0.5 s and diastolic phase of 0.5 s. As boundary conditions, the LHHM is constrained in space by fixed node sets at cut planes of the ascending aorta, pulmonary trunk, and superior vena cava.

2.3 TMVR modeling

The LHHM adopts the ABAQUS/Explicit solver for simulating the cardiac beat. The simulation begins with filling the LHHM with blood to a state consistent with being at 70% through the diastolic phase of the cardiac cycle (time of 0.5 s). Then, the implantation of the band ring is obtained by generating frictionless contact conditions between the band ring and the MV annulus. The presence of sutures is considered using several wires connecting the band ring periphery to the MV annulus in the radial direction. Then, the S3 Ultra was placed in the LHHM and crimped by a rigid dodecahedral surface gradually moved along the radial direction from the initial device diameter to the final diameter of 4.5 mm. Frictionless contact conditions were set between the crimping surface and the S3 Ultra while tie contact conditions were used to fix the skirt surfaces to the crimped THV device. Similarly, the balloon is deflated by radial displacement of a cylindrical crimper and constraining distal ends in all directions (Fig. 1B) (Pasta et al., 2020b). The crimped S3 Ultra and folded balloon was placed in the LHHM following manufacturer recommendations with 1/3 of S3 Ultra frame in the left atrium and the remaining part on the left ventricular chamber. To further investigate the interaction of the S3 Ultra with the human host, the case of a high implantation depth in the left atrium was also investigated. This was obtained by translating the device and implantation system of 5 mm in the left atrium. Frictionless contact conditions were used to replicate the interaction of S3 Ultra with the balloon surface.

In a third step, the S3 Ultra was expanded using the fluid-cavity-based approach to ensure a realistic volume-controlled inflation upon the nominal fluid volume of 17 ml. Balloon overexpansion may occur in clinical setting to increase the device adherence to the band ring. In this way, an additional simulation was developed increasing the fluid volume of 1 ml with respect to the reference one. The device expansion was carried out with the mitral valve at fully opened position to warrant the relative position of S3 Ultra system into the mitral valve annulus. The bioprosthetic valve leaflets were mapped on the device frame after the deployment process, and then the heart completed three cardiac cycles to reach a steady-state solution. Contacts among components were defined according to the general contact algorithm implemented in the LHHM.

2.3 Computational flow analysis

After TMVR simulation, deformed geometries of the left heart and deployed THV were exported at the end-systolic cardiac phase for computational fluid dynamic analysis. The inner heart volume was meshed with 3,715,183 tetrahedral elements using the ICEM CFD (v21.0, ANSYS Inc., Canonsburg, PA). Laminar flow condition and non-Newtonian viscosity described by the Carreau model were assumed (Pasta et al., 2017). Computational flow analysis was carried out using an implicit algorithm in FLUENT (v21, ANSYS Inc., Canonsburg, PA, USA). For boundary conditions (see Fig. 2), flow velocity inlets were set at each pulmonary vein and then split, assuming proportionality of each pulmonary vein cross-sectional area and mass balance conservation. For outflow, a pressure outlet profile was imposed at the aortic root of the LHHM using published data (Pasta et al., 2020b). Three cardiac beats were simulated to reduce instabilities related to the transient flow, and the last cycle was used for flow analysis.

3. Results

Figure 3 shows several steps of S3 Ultra deployment in the LHHM as the expandable balloon is inflated by the fluid-filling volume to guide the device anchoring. Both the band ring and mitral valve represent the key anchoring zones with the device being in contact first with the band ring (Fig. 3D). The S3 Ultra and balloon surface displaced the native mitral valve towards the myocardium, with the anterior mitral valve leaflet moving towards the native LVOT anatomy (Fig. 3E). It is also noted that the opening and closing of the mitral valve is reduced thanks to the presence of the virtual ischemic region near the papillary muscle (ie, reduced passive and active heart contractility). The last step shows the balloon filling phase at maximum expansion in the mitral position (Fig. 3F).

To evaluate the biomechanical performance of TMVR, the contact pressure and stent-anchoring contact area over one cardiac beat were computed for both the mitral valve and band ring (Fig. 4). For the band ring, both the contact pressure and area had a sharp rise during the S3 deployment and then decreased during cardiac beating. For the mitral valve, contact pressure was high during

the passive left ventricular filling. Fig. 4C also shows the opened and closed configurations of bioprosthetic valve leaflets at both end-systolic and end-diastolic cardiac phases.

Fig. 4D and E highlights the distribution of the mitral valve displacements and Von Mises stress distribution at the end-diastole. The anterior mitral valve leaflet experienced a peak displacement of 23 mm as compared to the closed configuration before device deployment. The leaflet free edge is mostly displaced to the interventricular septum as compared to those the mitral annulus constrained by the stiff band ring. The peak values of the Von Mises stress were observed near the mitral valve annulus as caused by anatomic constraints. No considerable changes were observed for mitral valve displacement and stress distributions during the cardiac beat (data not shown).

The neo-LVOT obstruction and resulting anatomic area were computed according to the workflow suggested by Blanke and collaborators (Fig. 5) [4]. We generated the geometric centerline of the aortic root and native LVOT anatomy, and then developed the cross-sectional plane perpendicular to the centerline in correspondence with the smallest neo-LVOT area that was formed by the S3 Ultra frame and the interventricular septum. The mean value of the neo-LVOT area over a cardiac beat was 367.7 mm^2, but the numerical simulation revealed a high dynamic behavior of device-related obstruction. Fig. 6 shows that the neo-LVOT area changed significantly over the cardiac beat, with nearly a 50% reduction at peak systolic myocardial contraction (end-systole) with respect to the relaxed myocardium (end-diastole). The comparative study using the stiff band ring, high implantation depth and balloon overexpansion highlighted different TMVR simulation outcomes (Fig. 7). Table 2 summarizes the changes of neo-LVOT area and contact pressure with respect to the reference LHHM model.

Fig. 8 shows the blood flow velocity disturbances and pressure distribution encompassing the neo-LVOT obstruction at the early systole. Hemodynamics evinced pronounced flow velocity near the periphery of interventricular septum confined by the implanted device. Nested helical flow was observed near the S3 skirt and the anterior mitral valve leaflet. A drop in the pressure field of 4.5 mmHg between the left ventricle and neo-LVOT region was computed.

4. Discussion

In this study, a realistic and high-fidelity computational tool of cardiac biomechanics was used to virtually simulate the transcatheter mitral valve-in-ring replacement and then investigate the hemodynamic and structural mechanics of LVOT obstruction. The most striking finding is the assessment of the dynamic behavior of the neo-LVOT area over the cardiac cycle, suggesting that the risk stratification of patients undergoing TMVR should not only be based on pre-TMVR imaging criteria at end-systole. This finding improves our understanding of the impact that LVOT obstruction has on THV performance and offers a computational approach to better assess the anatomic suitability of patients undergoing TMVR. Ultimately, this knowledge has the potential to enhance procedural planning to yield better clinical outcomes and to inform the way we design the next-generation of transcatheter heart valves.

LVOT obstruction is a major concern in TMVR, but limited data exist regarding its biomechanical implication on cardiac function. Major findings from computational analyses were related to the computational fluid dynamic in left ventricular geometries with obstructions idealized as a rigid wall protrusion (De Vecchi et al., 2018; Kohli et al., 2018). This approach made it possible to derive new metrics for quantifying the hemodynamic alteration near the LVOT region and its effect on cardiac function, as characterized by an increase in ventricular afterloads and a deterioration of systolic flow efficiency. Recently, fluid-solid interaction analysis was developed to first simulate the THV deployment and then evaluate the resulting hemodynamic environment (Pasta et al., 2020a). However, the computational simulation run until the deployment phase, thereby not considering the importance of the beating heart. Using the LHHM in the setting of TAVR, Ghosh and collaborators (Ghosh et al., 2020) found that if the simulation is stopped short upon the deployment phase, the anchoring behavior is unchanged as the device is virtually implanted at different heights. As the heart starts beating, the important interaction between the tissue and device frame can be realistically revealed to provide the performance of the implanted device in the aortic root. For pre-TMVR assessment of patient anatomic suitability, computer-aided-design (CAD) principles and 3D

printing of human models were implemented to predict the impact of LVOT obstruction (Wang et al., 2016). The workflow consisted of overlapping a cylindrical surface representing the THV geometry on the segmented left ventricular patient anatomy at end-systole and then measuring the neo-LVOT area using CAD tools. Different angles and implantation depths can be quickly obtained by manipulation (ie, rotation and translation) of the cylindrical device geometry in the left ventricle. The left heart is then manufactured in a rigid phantom to allow visual inspection of LVOT obstruction from the aortic root view. Though neo-LVOT area predictions were found in good agreement with those seen from post-TMVR imaging (Wang et al., 2018), this approach does not consider the interaction of the deforming myocardial wall with the stiff THV stent frame.

A careful CT-based analysis of anatomic features in a patient is therefore the standard approach to stratify patients at high risk of developing hemodynamic impairment associated with the neo-LVOT. Blanke and collaborators (Blanke et al., 2017) therefore developed a workflow to virtually implant the device model in the mitral valve and measure the smallest neo-LVOT area on the CT image. Subsequently, the predictive performance of the cutoff value of the neo-LVOT area for discriminating the risk of adverse events associated with the device elongation was demonstrated in several clinical reports . However, the CT-based analysis described by Blanke et al (Blanke et al., 2017) cannot consider the dynamic changes of the estimated neo-LVOT over the cardiac cycle. In this study, we demonstrated a remarkable change in the neo-LVOT area ranging from a maximum of 472.1 mm^2 at early systole to a minimum of 183.0 mm^2 at end-systole. The minimum value of neo-LVOT area is therefore close to the clinical cut-off of 170 mm^2. The comparative study demonstrated that role of band ring material properties, device overexpansion and suboptimal implantation depth on the resulting device performance. Low magnitude of neo-LVOT area at systole and diastole were found for the stiff band ring and balloon overexpansion, with lowest area measurements when the fluid-filling volume was increased. In a different way, a shift of the implantation depth towards the left atrium led to larger neo-LVOT area but lower contact pressure on the mitral valve than that shown by the reference model following manufacturer guidelines. We

316 also observed that the mitral valve displacement does not vary during cardiac beating and thus
317 speculate that the changes in the neo-LVOT area are mainly caused by the myocardial contraction
318 occurring during systole rather than a motion of the S3 device. During systolic contraction, the
319 contact pressure and anchoring area of the S3 device revealed a slightly increase due to the
320 compression of the surrounding tissue on the band ring surface. The latter serves as the key
321 anchoring zone while the mitral valve is primally displaced by the deployed device. When observed
322 from the aortic root, the S3 device is partially covered by the mitral valve, which, together with the
323 sealing skirt, can lead to hemodynamic alteration in the neo-LVOT region. Our computational flow
324 analysis revealed a sub-stenotic aortic stenotic flow and a pressure drop at the neo-LVOT region.
325 These parameters may allow for more accurate prediction of the LVOT obstruction in TMVR,
326 particularly for patients considered to have a borderline risk of obstruction. The implanted device
327 frame presented distorted cells likely caused by the fact that the S3 Ultra is not specifically
328 designed to treat the mitral valve, and this may prevent correct functioning. Clinical studies have
329 demonstrated the feasibility of TMVR with the S3 device (Babaliaros et al., 2021), but the long-term
330 outcome have been not addressed yet. Findings as here reported can be used as input to design
331 the next generation of THV with unique design features for TMVR procedures.

332

333 Though the most advanced cardiac tool was used for a deep investigation of the neo-LVOT
334 biomechanics, this study presents several limitations caused by the complexity of TMVR. The
335 LHHM anatomic geometry and function are likely different from those of the patient undergoing
336 TMVR. A fully-coupled fluid-solid interaction analysis for assessing the hemodynamic disturbances
337 induced by LVOT obstruction is highly desirable, albeit hugely challenging. The mitral valve leaflets
338 of LHHM are relatively short even if they are considered in the normal physiological range. The last
339 version of LHHM allows the change of mitral valve geometry and mesh but only the left atrial and
340 ventricular chambers are implemented in the numerical cardiac tool. A frictionless contact condition
341 was assumed between the device and human host while literature data suggests friction coefficient
342 in the range of 0.1 and 0.2. Most importantly, the present computational simulation lacks of a

validation and verification assessment to assess the accuracy of the model predictions. This is not feasible as the LHHM is based on ideal adult geometry. A comparative analysis with measurements done by post-TMVR imaging demonstrates that our prediction of the neo-LVOT area agrees well with data reported by Yoon et al (Yoon et al., 2019), who suggested values of neo-LVOT area ranging from 220 mm2 to 430 mm2 in a large cohort of valve-in-ring patient cases. Verification on the mesh and model setting should be carried out to establish the simulation credibility and reliability. Though element convergence was not performed, the LHHM was found to provide a steady-state solution with stable stress values after three cardiac cycles with the mesh volume here used. The constitutive model of passive and active contraction as well as the electrical model were validated against experimental data. Finally, current validation studies of LHHM have shown a good agreement with clinical data in terms of left and right ventricular ejection, maximum and minimum blood pressure for the four heart chambers and maximum left ventricular apex-base shorterning (Baillargeon et al., 2014).

5. Conclusion

Our findings are relevant to a) reduce the gap in the knowledge of TMVR when THVs are used off label for mitral implantation, and b) provide relevant structural and hemodynamic metrics to develop THVs specifically designed to accommodate the challenging mitral valve function. Future studies in patient-specific geometries including different mitral valve morphologies ~~different sizes of mitral valve leaflets and stiff versus flexible band rings~~ will help to achieve better translational clinical value by enhancing the pre-TMVR planning in borderline patient anatomy.

Acknowledgements

This study was funded by the grant “Sim4SAPIEN” from the Edwards Lifesciences SA (THV-I20-532). The authors thank the Living Heart Project community and Dassault Systemes Simulia

Corporation for supporting the computational modeling development. Mrs Catalano thanks the SimInSitu project (No 101017523) for supporting her research fellowship.

Conflict of interest statement

The authors declare that they have no known competing financial interests or personal relationships that could have appeared to influence the work reported in this paper.

References

Auricchio, F., Conti, M., Morganti, S., Reali, A., 2014. Simulation of transcatheter aortic valve implantation: a patient-specific finite element approach. Computer methods in biomechanics and biomedical engineering 17, 1347-1357.

Babaliaros, V.C., Lederman, R.J., Gleason, P.T., Khan, J.M., Kohli, K., Sahu, A., Rogers, T., Bruce, C.G., Paone, G., Xie, J.X., Kamioka, N., Condado, J.F., Byku, I., Perdoncin, E., Lisko, J.C., Greenbaum, A.B., 2021. The Art of SAPIEN 3 Transcatheter Mitral Valve Replacement in Valve-in-Ring and Valve-in-Mitral-Annular-Calcification Procedures. JACC. Cardiovascular interventions 14, 2195-2214.

Bailey, J., Curzen, N., Bressloff, N.W., 2016. Assessing the impact of including leaflets in the simulation of TAVI deployment into a patient-specific aortic root. Computer methods in biomechanics and biomedical engineering 19, 733-744.

Baillargeon, B., Costa, I., Leach, J.R., Lee, L.C., Genet, M., Toutain, A., Wenk, J.F., Rausch, M.K., Rebelo, N., Acevedo-Bolton, G., Kuhl, E., Navia, J.L., Guccione, J.M., 2015. Human Cardiac Function Simulator for the Optimal Design of a Novel Annuloplasty Ring with a Sub-valvular Element for Correction of Ischemic Mitral Regurgitation. Cardiovasc Eng Technol 6, 105-116.

Baillargeon, B., Rebelo, N., Fox, D.D., Taylor, R.L., Kuhl, E., 2014. The Living Heart Project: A robust and integrative simulator for human heart function. Eur J Mech A Solids 48, 38-47.

Bapat, V., Rajagopal, V., Meduri, C., Farivar, R.S., Walton, A., Duffy, S.J., Gooley, R., Almeida, A., Reardon, M.J., Kleiman, N.S., Spargias, K., Pattakos, S., Ng, M.K., Wilson, M., Adams, D.H., Leon, M., Mack, M.J., Chenoweth, S., Sorajja, P., Intrepid Global Pilot Study, I., 2018. Early Experience With New Transcatheter Mitral Valve Replacement. J Am Coll Cardiol 71, 12-21.

Blanke, P., Naoum, C., Dvir, D., Bapat, V., Ong, K., Muller, D., Cheung, A., Ye, J., Min, J.K., Piazza, N., Theriault-Lauzier, P., Webb, J., Leipsic, J., 2017. Predicting LVOT Obstruction in Transcatheter Mitral Valve Implantation: Concept of the Neo-LVOT. JACC. Cardiovascular imaging 10, 482-485.

Castillo-Sang, M., Guthrie, T.J., Moon, M.R., Lawton, J.S., Maniar, H.S., Damiano, R.J., Jr., Silvestry, S.C., 2015. Outcomes of repeat mitral valve surgery in patients with pulmonary hypertension. Innovations (Phila) 10, 120-124.

De Vecchi, A., Marlevi, D., Nordsletten, D.A., Ntalas, I., Leipsic, J., Bapat, V., Rajani, R., Niederer, S.A., 2018. Left ventricular outflow obstruction predicts increase in systolic pressure gradients and blood residence time after transcatheter mitral valve replacement. Scientific reports 8, 15540.

Ghosh, R.P., Marom, G., Bianchi, M., D'Souza, K., Zietak, W., Bluestein, D., 2020. Numerical evaluation of transcatheter aortic valve performance during heart beating and its post-deployment fluid-structure interaction analysis. Biomechanics and modeling in mechanobiology 19, 1725-1740.

Guccione, J.M., Moonly, S.M., Moustakidis, P., Costa, K.D., Moulton, M.J., Ratcliffe, M.B., Pasque, M.K., 2001. Mechanism underlying mechanical dysfunction in the border zone of left ventricular aneurysm: A finite element model study. Annals of Thoracic Surgery 71, 654-662.

Guccione, J.M., Salahieh, A., Moonly, S.M., Kortsmit, J., Wallace, A.W., Ratcliffe, M.B., 2003. Myosplint decreases wall stress without depressing function in the failing heart: a finite element model study. Ann Thorac Surg 76, 1171-1180; discussion 1180.

Holzapfel, G.A., Ogden, R.W., 2009. Constitutive modelling of passive myocardium: a structurally based framework for material characterization. Philos Trans A Math Phys Eng Sci 367, 3445-3475.

Kohli, K., Wei, Z.A., Yoganathan, A.P., Oshinski, J.N., Leipsic, J., Blanke, P., 2018. Transcatheter Mitral Valve Planning and the Neo-LVOT: Utilization of Virtual Simulation Models and 3D Printing. Current treatment options in cardiovascular medicine 20, 99.

Kunzelman, K.S., Cochran, R.P., Chuong, C., Ring, W.S., Verrier, E.D., Eberhart, R.D., 1993. Finite element analysis of the mitral valve. The Journal of heart valve disease 2, 326-340.

May-Newman, K., Yin, F.C., 1995. Biaxial mechanical behavior of excised porcine mitral valve leaflets. Am J Physiol 269, H1319-1327.

Morganti, S., Brambilla, N., Petronio, A.S., Reali, A., Bedogni, F., Auricchio, F., 2016. Prediction of patient-specific post-operative outcomes of TAVI procedure: The impact of the positioning strategy on valve performance. J Biomech 49, 2513-2519.

Muller, D.W.M., Farivar, R.S., Jansz, P., Bae, R., Walters, D., Clarke, A., Grayburn, P.A., Stoler, R.C., Dahle, G., Rein, K.A., Shaw, M., Scalia, G.M., Guerrero, M., Pearson, P., Kapadia, S., Gillinov, M., Pichard, A., Corso, P., Popma, J., Chuang, M., Blanke, P., Leipsic, J., Sorajja, P., Tendyne Global Feasibility Trial, I., 2017. Transcatheter Mitral Valve Replacement for Patients With Symptomatic Mitral Regurgitation: A Global Feasibility Trial. J Am Coll Cardiol 69, 381-391.

Muller, D.W.M., Sorajja, P., Duncan, A., Bethea, B., Dahle, G., Grayburn, P., Babaliaros, V., Guerrero, M., Thourani, V.H., Bedogni, F., Denti, P., Dumonteil, N., Modine, T., Jansz, P., Chuang, M.L., Blanke, P., Leipsic, J., Badhwar, V., 2021. 2-Year Outcomes of Transcatheter Mitral Valve Replacement in Patients With Severe Symptomatic Mitral Regurgitation. J Am Coll Cardiol 78, 1847-1859.

Pasta, S., Cannata, S., Gentile, G., Agnese, V., Pilato, M., Gandolfo, C., 2020a. Simulation of left ventricular outflow tract (LVOT) obstruction in transcatheter mitral valve-in-ring replacement. Med Eng Phys 82, 40-48.

Pasta, S., Cannata, S., Gentile, G., Di Giuseppe, M., Cosentino, F., Pasta, F., Agnese, V., Bellavia, D., Raffa, G.M., Pilato, M., Gandolfo, C., 2020b. Simulation study of transcatheter heart valve implantation in patients with stenotic bicuspid aortic valve. Med Biol Eng Comput.

Pasta, S., Gentile, G., Raffa, G.M., Scardulla, F., Bellavia, D., Luca, A., Pilato, M., Scardulla, C., 2017. Three-dimensional parametric modeling of bicuspid aortopathy and comparison with computational flow predictions. Artif Organs 41, E92-E102.

Walker, J.C., Ratcliffe, M.B., Zhang, P., Wallace, A.W., Fata, B., Hsu, E.W., Saloner, D., Guccione, J.M., 2005. MRI-based finite-element analysis of left ventricular aneurysm. Am J Physiol-Heart C 289, H692-H700.

Wang, D.D., Eng, M., Greenbaum, A., Myers, E., Forbes, M., Pantelic, M., Song, T., Nelson, C., Divine, G., Taylor, A., Wyman, J., Guerrero, M., Lederman, R.J., Paone, G., O'Neill, W.,

2016. Predicting LVOT Obstruction After TMVR. JACC. Cardiovascular imaging 9, 1349-1352.

Wang, D.D., Eng, M.H., Greenbaum, A.B., Myers, E., Forbes, M., Karabon, P., Pantelic, M., Song, T., Nadig, J., Guerrero, M., O'Neill, W.W., 2018. Validating a prediction modeling tool for left ventricular outflow tract (LVOT) obstruction after transcatheter mitral valve replacement (TMVR). Catheter Cardio Inte 92, 379-387.

Whisenant, B., Kapadia, S.R., Eleid, M.F., Kodali, S.K., McCabe, J.M., Krishnaswamy, A., Morse, M., Smalling, R.W., Reisman, M., Mack, M., O'Neill, W.W., Bapat, V.N., Leon, M.B., Rihal, C.S., Makkar, R.R., Guerrero, M., 2020. One-Year Outcomes of Mitral Valve-in-Valve Using the SAPIEN 3 Transcatheter Heart Valve. JAMA cardiology 5, 1245-1252.

Wu, S., Chai, A., Arimie, S., Mehra, A., Clavijo, L., Matthews, R.V., Shavelle, D.M., 2018. Incidence and treatment of severe primary mitral regurgitation in contemporary clinical practice. Cardiovasc Revasc Med 19, 960-963.

Yoon, S.H., Bleiziffer, S., Latib, A., Eschenbach, L., Ancona, M., Vincent, F., Kim, W.K., Unbehaum, A., Asami, M., Dhoble, A., Silaschi, M., Frangieh, A.H., Veulemans, V., Tang, G.H.L., Kuwata, S., Rampat, R., Schmidt, T., Patel, A.J., Nicz, P.F.G., Nombela-Franco, L., Kini, A., Kitamura, M., Sharma, R., Chakravarty, T., Hildick-Smith, D., Arnold, M., de Brito, F.S., Jr., Jensen, C., Jung, C., Jilaihawi, H., Smalling, R.W., Maisano, F., Kasel, A.M., Treede, H., Kempfert, J., Pilgrim, T., Kar, S., Bapat, V., Whisenant, B.K., Van Belle, E., Delgado, V., Modine, T., Bax, J.J., Makkar, R.R., 2019. Predictors of Left Ventricular Outflow Tract Obstruction After Transcatheter Mitral Valve Replacement. JACC. Cardiovascular interventions 12, 182-193.

Figure Captions

Fig 1 (A) LHHM model with insets showing the mitral valve and chordae as well as the ischemic region (red color) of the left ventricle generated for developing the mitral valve regurgitation; (B) unfolded and folded balloon surface model and crimped S3 model

Fig 2 Flow boundary conditions at both inlets and outlets; the inflow velocity is a representative flow profile imposed on the pulmonary vein while other inflow profiles branches are scaled version of the present one and are obtained from proportionality of each pulmonary vein cross-sectional area and mass balance conservation. For outlet, the physiological pressure profile seen by the left ventricle was applied to aortic root outflow surface.

Fig 3 Various steps of the S3 THV deployment for the mitral valve in-ring treatment

Fig 4 Profiles of the contact pressure and area exerted on both the (A) band ring and (B) mitral valve; (C) opened and closed configuration of S3 valve leaflets as mapped after the deployment phase, map of (D) displacement and (E) Mises stress distribution of mitral valve at end-systole

Fig 5 Different 3D views of the neo-LVOT area (top left shows the calculation approach) at end-systole

Fig 6 Profiles of the neo-LVOT area changes over the cardiac beat; insets shows neo-LVOT area at end-systole and end-diastole

Fig 7 Changes in the TMVR simulations in case of a stiff band, balloon overexpansion and high implantation depth.

Fig 8 End-systolic distribution of blood-flow velocity showing subaortic flow stenosis in the neo-LVOT and blood pressure with the drop computed between the left ventricle neo-LVOT area

Table 1: Material parameters of mitral valve, left ventricle and ischemic region

	a (MPa)	b	a_f (MPa)	b_f	a_s (MPa)	b_s	a_{fs} (MPa)	b_{fs}	C_{a0} (μmol/L)
Mitral Valve	8.7e-4	2.7	5.0e-4	12.0	3.8e-3	7.6e-1	3.8e-3	7.6e-1	
Left ventricle	4.0e-1	12.0	5.0e-1	5.0	2.0e-1	2.0	1.1e-2	2.0	2.66
Ischemic region	5.2e-1	12.0	5.0e-1	5.0	2.0e-1	2.0	1.1e-2	2.0	2.12

Table 2: Comparison of neo-LVOT area values among different parametric models

	Neo-LVOT area (mm^2)		Contact Pressure (MPa)	
	Max	Min	Ring	Mitral Valve
Reference Model	472.1	183.0	28.2	26.7
Stiff Band Ring	455.8	165.7	41.6	32.5
Balloon Overexpansion	434.6	151.4	32.8	29.4
High Implantation Depth	495.6	201.2	30.5	22.3

513 **Fig. 1**

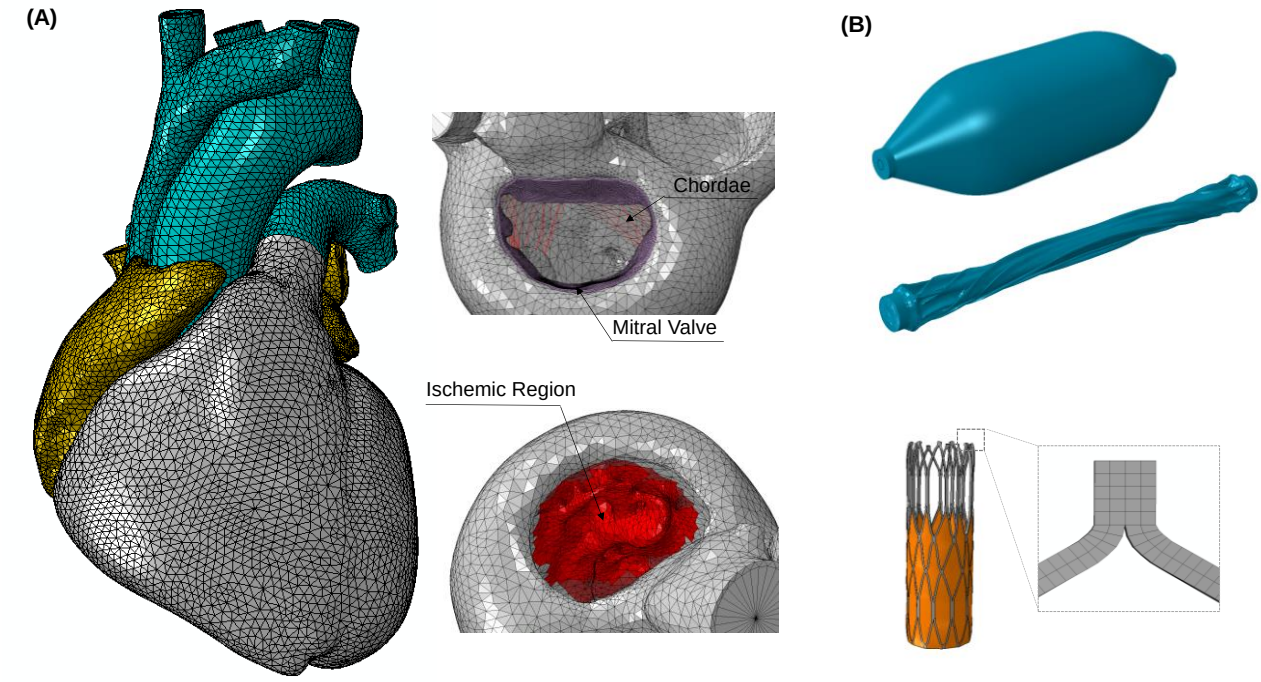

514

515

516

517 **Fig.2**

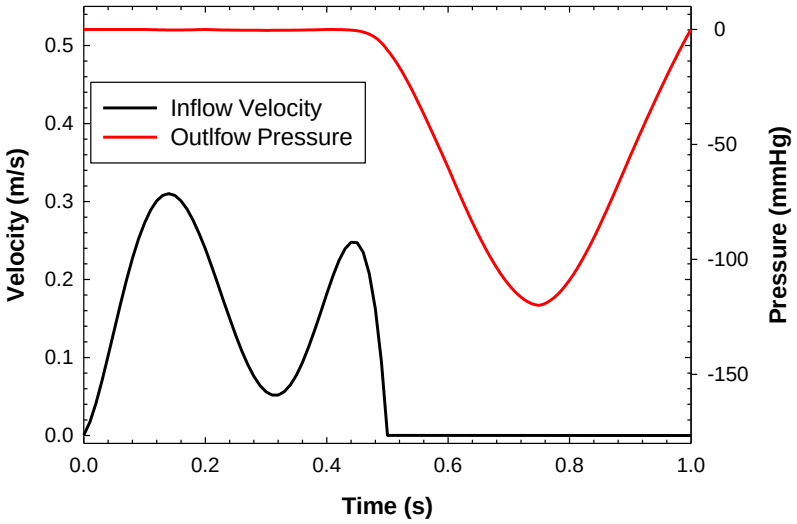
Inflow Velocity
Outlfow Pressure
Velocity (m/s)
Pressure (mmHg)
Time (s)
0.0
0.1
0.2
0.3
0.4
0.5
0
-50
-100
-150
0.0
0.2
0.4
0.6
0.8
1.0

518

519 **Fig.3**

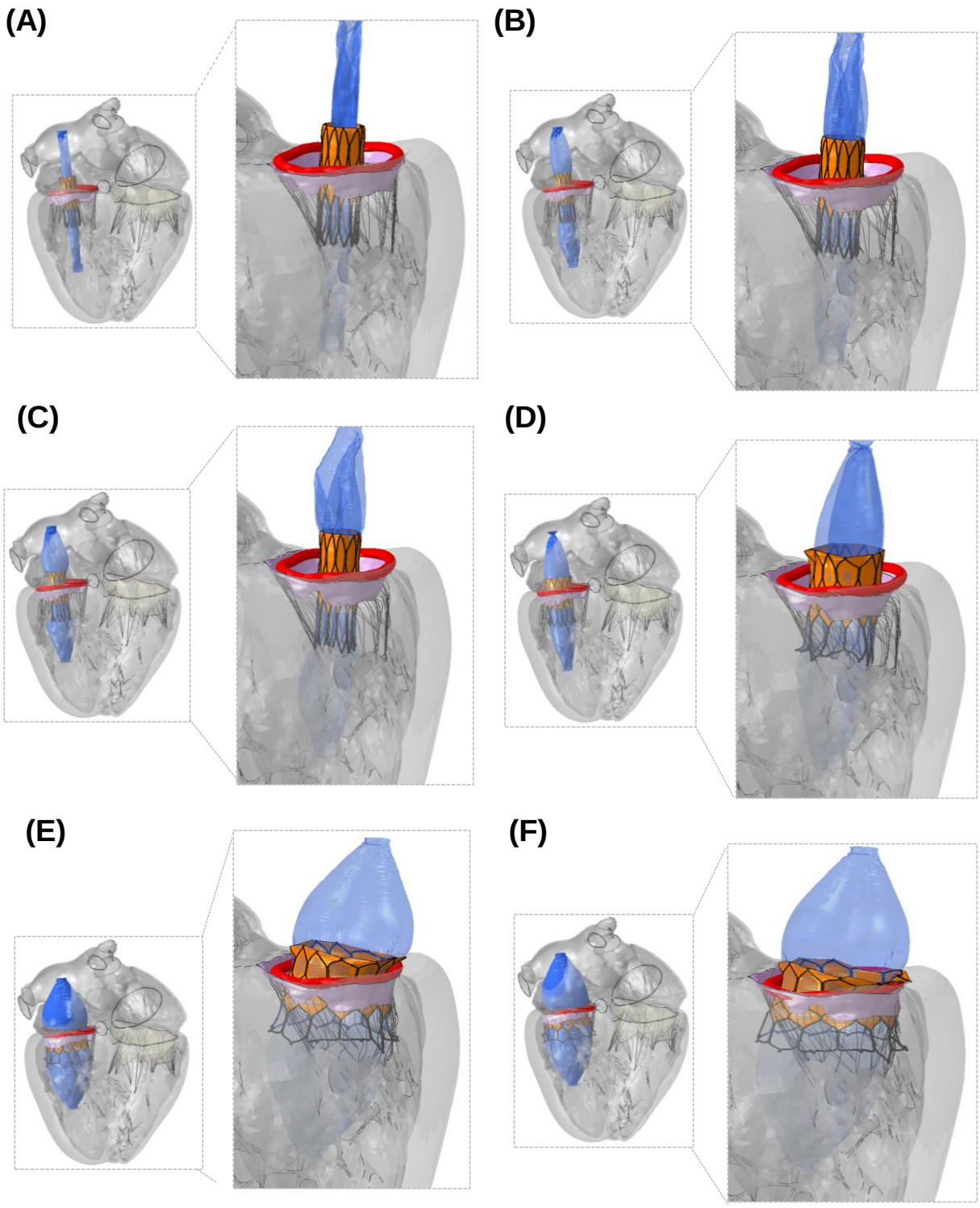

520

521

522 **Fig. 4**

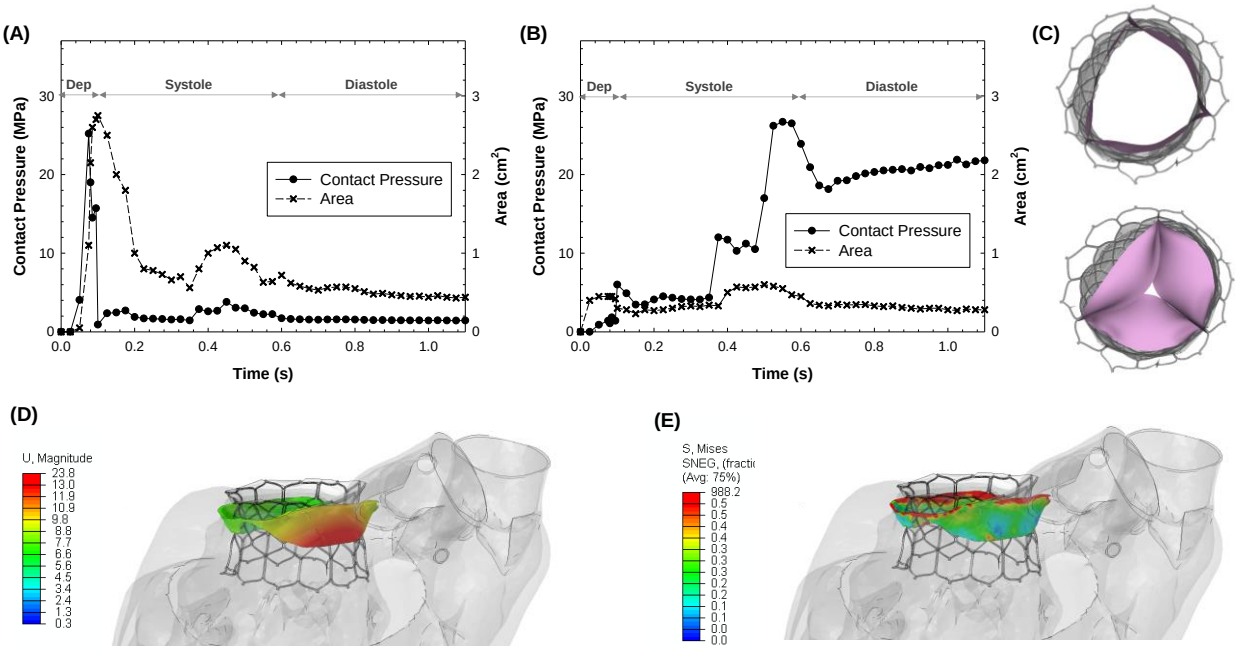

523

524

525

526 **Fig. 5**

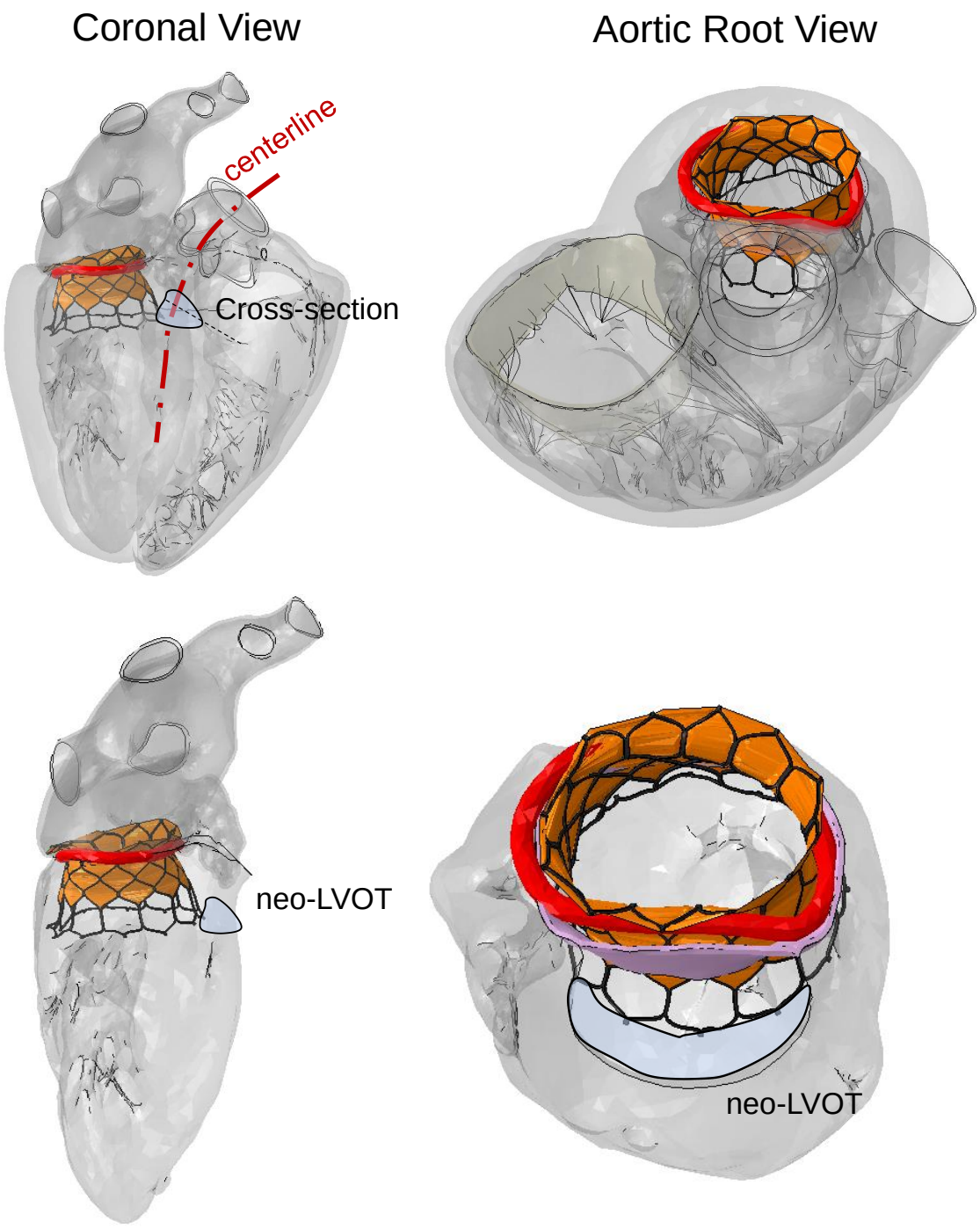

527

528

529 **Fig. 6**

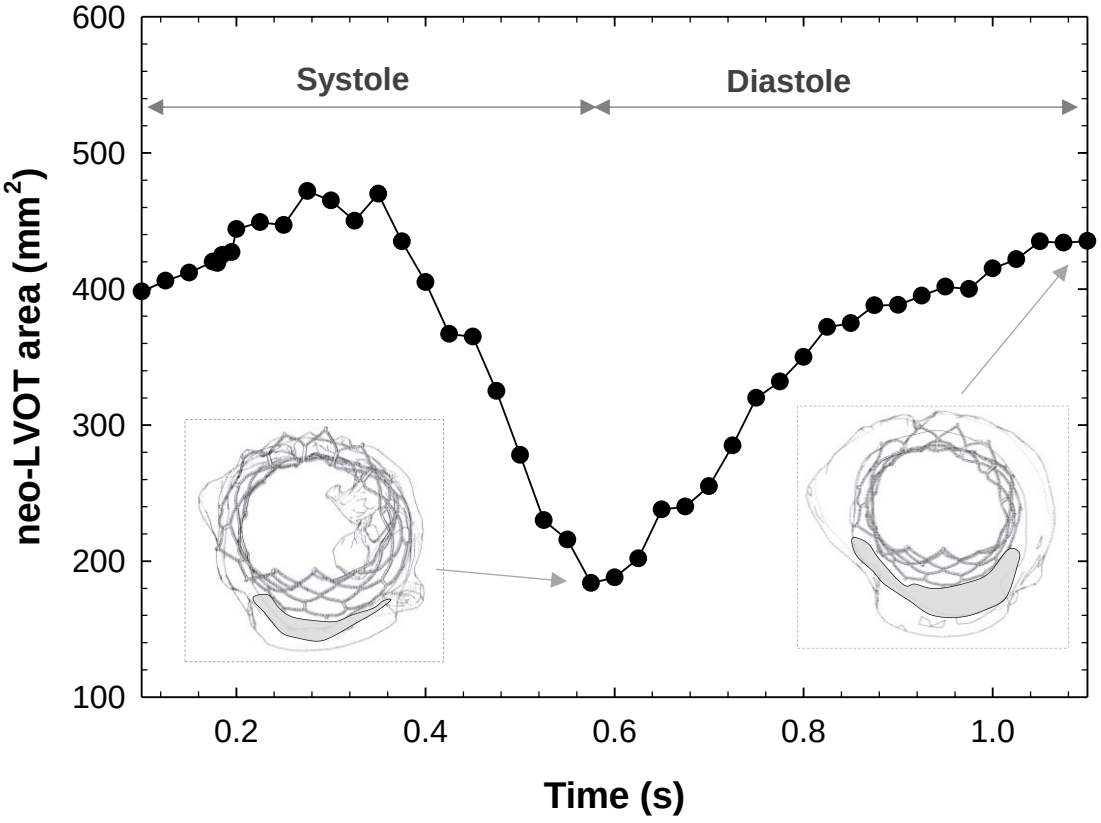

530

531

532

533 **Fig. 7**

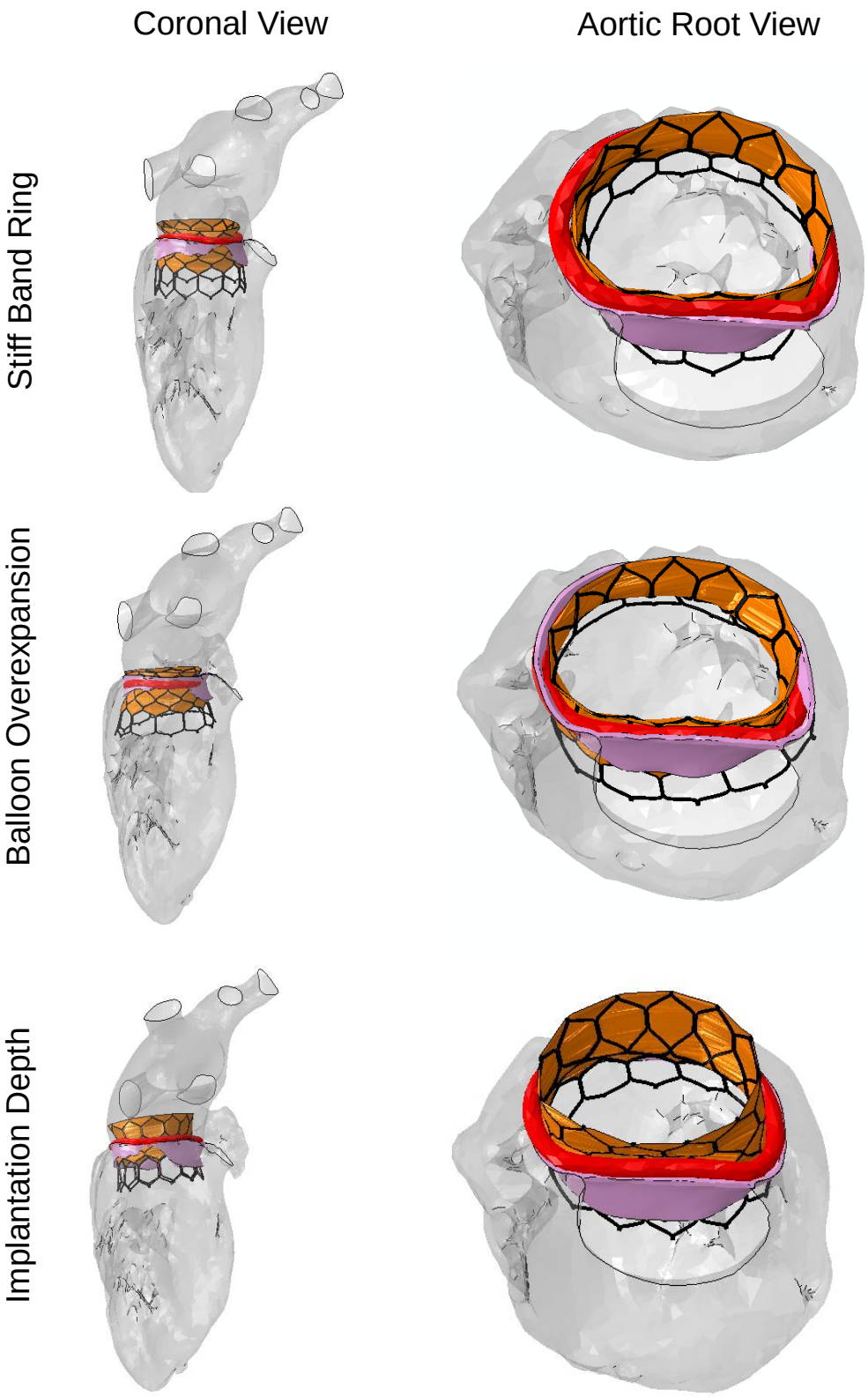
Coronal View
Aortic Root View
Stiff Band Ring
Balloon Overexpansion
Implantation Depth

534

Fig. 8

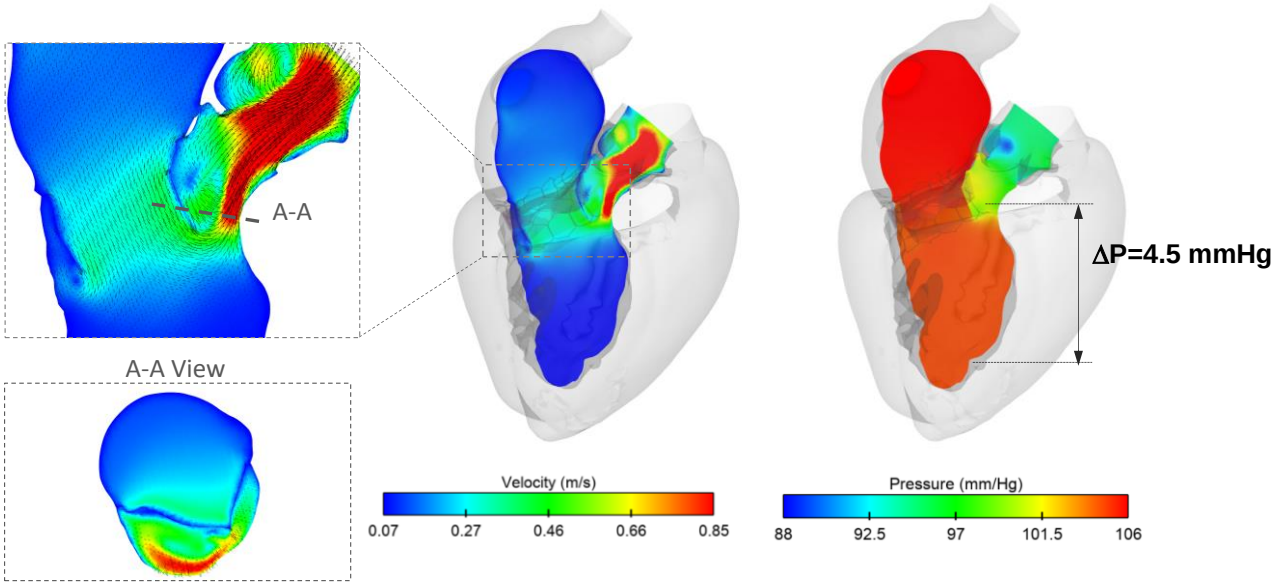
A-A
A-A View
Velocity (m/s)
0.07
0.27
0.46
0.66
0.85
Pressure (mm/Hg)
88
92.5
97
101.5
106
ΔP=4.5 mmHg

Dear Editor,

On the behalf of all authors, the present letter asserts that authors did not have any financial and personal relationships with other people or organisations that could inappropriately influence (bias) their work.

Best Regards,

Salvatore Pasta, Ph.D.,
Università di Palermo
Viale delle Scienze
Italy